MATHEMATICAL MODELING AND CHARACTERIZATION OF THE EFFECT OF QUORUM SENSING REGULATED T6SS KILLING ON BIOFILM STRUCTURE

ABIGAIL EZELL, DARWIN NESHEIM, AND KEVIN SWEET

Main Advisor: Blessing O. Emerenini
Secondary Advisor: Ricardo N. G. Reyes Grimaldo
Oregon State University

Abstract. Bacterial interactions heavily impact how a biofilm forms, and how bacteria communicate impacts how they interact. One way that bacteria can communicate is through the production and sensing of quorum sensing molecules which regulate certain genetic expressions. It was our focus to model and analyze the relationship between quorum sensing regulated Type VI Secretion System (T6SS) mediated killing in two strains of *Agrobacterium tumefaciens* and biofilm structure. We constructed a deterministic two dimensional model that held the rate of quorum sensing molecule production constant in order to illustrate basic interactions between two bacterial strains and the effect that such interactions have on the biofilm's development. By adding another dimension to our model we can more realistically show the effects that quorum sensing regulated T6SS mediated killing has on the biofilm's structure based on the current state of the biofilm. This work illustrates how quorum sensing T6SS mediated killing contributes to overall biofilm structure.

1. Introduction

Biofilms are communities of bacteria that attach to surfaces. They can comprise one or multiple species of bacteria. The bacteria that live in biofilms interact with each other in a number of ways, varying by the type of bacteria: they can produce public goods to aid other cells, or they can compete with one another for space and access to nutrients [2]. Cells can also communicate with each other via quorum

Date: August 14, 2020.

This work was done during the Summer of 2020 REU program in Mathematics and Theoretical Computer Science at Oregon State University supported by NSF grant DMS-1757995.

sensing. One way bacteria work to gain advantages for themselves is by killing other nearby cells. A mechanism used for this purpose is the Type VI Secretion System (T6SS), which is regulated in part by quorum sensing in many bacteria [3, 11, 12, 13, 19, 22, 23]. One such species is *Agrobacterium tumefaciens*.

Agrobacterium tumefaciens is a species of bacteria that causes crown gall disease in many different plant species. It forms a biofilm on the plant host it is infecting [15]. We are interested in the interaction of different strains of this bacteria within the biofilm, with a particular focus on T6SS-mediated killing and quorum sensing.

Quorum sensing is a method by which bacteria can communicate with each other. This is done through the use of quorum sensing signaling molecules called autoinducers produced by the bacteria. Each cell produces this molecule on its own. In low numbers, the autoinducer has no effect, but as the number of bacteria in a biofilm increases, so too does the amount of the autoinducer. Once a certain threshold concentration of autoinducer is reached, the gene expression of the bacteria changes. Effects of this change in gene expression can include production of secreted toxins, biofilm matrix components and public goods [1, 16]. *A. tumefaciens* uses an acylated homoserine lactone (AHL) as its quorum sensing molecule [4]. The system that is of interest to us that is regulated by quorum sensing is the Type VI Secretion System in *A. tumefaciens*.

The Type VI Secretion System is a multi-protein complex that delivers effectors into neighboring eukaryotic or prokaryotic cells [5, 10, 9]. The T6SS is regulated by quorum sensing in many bacteria [3, 13, 22, 12, 11, 19, 23]. In addition to quorum sensing regulation, there are other factors that play into T6SS killing. For instance, there is a regulatory cascade of molecules that influence T6SS killing [6, 20]. In our paper, we will only be focusing on the effects of quorum sensing on T6SS-mediated killing.

Some other models of biofilms have examined the role of T6SS-mediated killing on biofilm growth and structure, such as those in [14] and [21]. The models in [14] examine the role of T6SS-mediated killing as it relates to the competition between strains of bacteria for shared goods. The model in [21] looks at the relationship between T6SS-mediated killing and growth inhibitors. Both of these modelling projects found that an initially well-mixed biofilm will form clusters of the same strain of bacteria.

However, neither considered the role of quorum sensing regulated T6SS-mediated killing in the development of the biofilm.

In our paper, we present a model that accurately describes the development of a biofilm that consists of two different strains of *A. tumefaciens*. In particular, our model incorporates bacterial growth, T6SS-mediated killing, and quorum sensing. Our models are deterministic models as ordinary differential equations (ODEs). As this is the first model that we're aware of that incorporates T6SS-mediated killing as it relates to quorum sensing, the deterministic model gives us more control over the system to investigate the dynamics we are interested in. Some research questions we are considering are the following:

- *What effect does quorum sensing regulated T6SS-mediated killing by* Agrobacterium tumefaciens *have on biofilm structure?*
- *Why is it beneficial for different strains of* Agrobacterium tumefaciens *to regulate T6SS-mediated killing through quorum sensing?*

We analyze our models using phase plane analysis, stability analysis, sensitivity analysis, and numerical simulation. We use MATLAB for our simulations.

2. Deterministic Models

Basic Assumptions. To better understand the relationship between quorum sensing and T6SS-mediated killing and the impacts of this relationship on the biofilm, we have developed several mathematical models. We are considering a biofilm composed of two bacterial strains, A and B. Both strains are capable of T6SS-mediated killing, so any bacterium has the potential to kill a bacterium of the other strain upon direct cell-to-cell contact. Our models take into account bacterial growth, bacterial death, T6SS-mediated killing, and quorum sensing's influence on T6SS-mediated killing.

We are assuming that quorum sensing positively regulates the T6SS mechanism; that is, quorum sensing induces activation of transcription factors that then initiate construction of the T6SS apparatus. This assumption is consistent with [11, 13], and [14]. Using this assumption, we expect to see more T6SS-mediated killing as the concentration of the autoinducer increases.

We also assume that the production rate of the autoinducer is governed by the local concentration of the autoinducer, as in [7]. The autoinducer is produced at a baseline rate until a specific threshold concentration is reached, after which the

production rate increases. Underlying this assumption is the idea that bacterial cells switch from a down-regulated to an up-regulated state once the concentration of the autoinducer is large enough, as [7] claims. A concentration of the autoinducer that is greater than the threshold will signal bacteria to increase production of the autoinducer.

Our final assumption is related to the movement of the biological components of our models. A biofilm is a dense living environment. As a result, factors such as cell-to-cell contact, cell-to-cell adhesion, and constriction caused by the extracellular polymeric substance will no doubt have an effect on bacterial motility. However, we follow the lead of [14] and [21] by assuming that density-dependent diffusion is a reasonable way to approximate cell movement. The autoinducer is also assumed to move solely through diffusion, as in [7].

2.1. **Governing Equations.** Putting our assumptions together, we have formulated three distinct but related models for biofilm growth - one two-dimensional ODE model, one three-dimensional ODE model, and one PDE model.
Our dependent variables are A, B, and Q, where A and B represent the volume fraction of bacterial strain A and B respectively, and Q represents the concentration of the dissolved autoinducer (Note that Q is an independent variable in Model 1).

2.2. **Model 1 - Simple ODE model for bacterial interaction.** Our first model closely resembles the system of ordinary differential equations set forth in [14]. We include terms for bacterial growth, r_1A and r_2B; unlike [14], we allow for the possibility of different growth rates. Bacterial death can happen as a result of interactions between strains or within one strain; this type of bacterial morbidity is captured by the terms $s_1A(A+B)$ and $s_2B(A+B)$. We deviate from [14] by allowing $s_1 \neq s_2$. We decided to vary r and s between strains in order to compare our findings with existing models. Finally, we capture quorum sensing regulated T6SS-mediated killing with the terms $\frac{Q^n}{\tau^n+Q^n}\alpha_{AB}AB$ and $\frac{Q^n}{\tau^n+Q^n}\alpha_{BA}AB$. The parameters α_{AB} and α_{BA} represent the rate at which strain B kills strain A and the rate at which strain A kills strain B, respectively. The coefficients $\frac{Q^n}{\tau^n+Q^n}$ and $\frac{Q^n}{\tau^n+Q^n}$ are included to

represent the influence of quorum sensing on T6SS-mediated killing. A simple two-dimensional ODE model is helpful for looking at the ways in which the variables and parameters in our model affect one another, as well as the overall system. With this model, we can easily conduct a sensitivity analysis to determine which parameters have the greatest effect on the behavior of the system. Additionally, note that Q is a parameter in Model 1, while it is a variable in Models 2 and 3. We have more control over Q as a parameter, allowing us to clearly see the state of the system for different concentrations of the autoinducer. The model reads as follows:

$$\frac{\mathrm{d}}{\mathrm{d}t}A = A\left(r_1 - s_1(A+B) - \frac{Q^n}{\tau^n + Q^n}\alpha_{AB}B\right) \tag{1}$$

$$\frac{\mathrm{d}}{\mathrm{d}t}B = B\left(r_2 - s_2(A+B) - \frac{Q^n}{\tau^n + Q^n}\alpha_{BA}A\right) \tag{2}$$

The schematic diagram in Figure 1 illustrates the action of each term on the relevant bacterial strain.

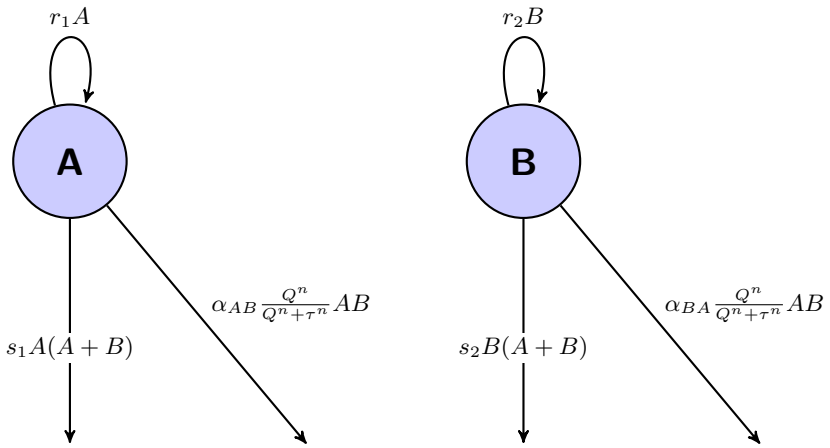

FIGURE 1. Schematic diagram for the 2D ODE model

To non-dimensionalize this model we need only rescale time, so we let $T = \frac{t}{\delta}$ where T is dimensionless and δ is a scaling parameter. By substituting for t and multiplying

by δ, the model now reads

$$\frac{\mathrm{d}}{\mathrm{d}T}A = \delta\left(r_1 A - s_1 A(A+B) - \frac{Q^n}{\tau^n + Q^n}\alpha_{AB}AB\right) \tag{3}$$

$$\frac{\mathrm{d}}{\mathrm{d}T}B = \delta\left(r_2 B - s_2 B(A+B) - \frac{Q^n}{\tau^n + Q^n}\alpha_{BA}AB\right) \tag{4}$$

where $\delta = \dfrac{1}{r_1 + r_2}$.

2.2.1. *Boundary behavior.* Since A and B are defined as volume fractions, we obtain the restrictions $0 \leq A, B \leq 1$. Thus, the set of positive real numbers of our state space is given by $\Omega = \{(A, B) \in \mathbb{R}^2 | 0 \leq A \leq 1, 0 \leq B \leq 1\}$. We analyze system (1) - (2) on the A and B axes as well as the lines $A = 1$ and $B = 1$ in order to confirm that solutions on the boundary always either stay on the boundary or point towards the interior of the state space.

On the A-axis, we have $B = 0$, so $\frac{\mathrm{d}}{\mathrm{d}t}B = 0$. Similarly, on the B-axis, we have $A = 0$, so $\frac{\mathrm{d}}{\mathrm{d}t}A = 0$. Therefore, solutions that lie on either the A-axis or B-axis will stay on the boundary.

When $B = 1$, we obtain $\dfrac{\mathrm{d}}{\mathrm{d}t}B = r_2 - s_2(A+1) - \dfrac{\alpha BAQ^n A}{Q^n + \tau^n}$. In order for solutions on the line $B = 1$ to remain in the state space, we need $\dfrac{\mathrm{d}}{\mathrm{d}t}B \leq 0$. Algebraic manipulation yields the equivalent condition $A \geq \dfrac{r_2 - s_2}{s_2 + \frac{\alpha_{BA}Q^n}{Q^n + \tau^n}}$. Now, observe that $\left(0, \dfrac{r_2}{s_2}\right)$ is a steady state of the system (more details about steady states are presented later, in the results section), so we need to ensure that $\left(0, \dfrac{r_2}{s_2}\right) \in \Omega$. Given that all parameters are nonnegative, this occurs when $\dfrac{r_2}{s_2} \leq 1$, which we can rearrange to yield $r_2 - s_2 \leq 0$. Returning to the condition on A, we see that $\dfrac{r_2 - s_2}{s_2 + \frac{\alpha_{BA}Q^n}{Q^n + \tau^n}}$ has a denominator that is always positive and a numerator that is less than or equal to zero. Since A cannot be negative, we see that $A \geq \dfrac{r_2 - s_2}{s_2 + \frac{\alpha_{BA}Q^n}{Q^n + \tau^n}}$ always holds. Hence, any solution on the line $B = 1$ will either stay on the boundary or point toward the interior of the state space.

Finally we examine the behavior of solutions on the line $A = 1$. We require that solutions satisfy $\frac{\mathrm{d}}{\mathrm{d}t}A|_{A=1} = r_1 - s_1(1+B) - \frac{\alpha_{AB}Q^nB}{Q^n+\tau^n} \leq 0$. Algebraic manipulation yields the equivalent condition $B \geq \frac{r_1 - s_1}{s_1 + \frac{\alpha_{AB}Q^n}{Q^n+\tau^n}}$. Observe that $\left(\frac{r_1}{s_1}, 0\right)$ is a steady state of the system. To ensure that the point $\left(\frac{r_1}{s_1}, 0\right)$ lies on the boundary, we need $\frac{r_1}{s_1} \leq 1$ to hold. Using an analogous argument as above, this condition implies that $r_1 - s_1 \leq 0$, which in turn implies that $\frac{r_1 - s_1}{s_1 + \frac{\alpha_{AB}Q^n}{Q^n+\tau^n}} \leq 0$. Since B cannot be negative, the condition $B \geq \frac{r_1 - s_1}{s_1 + \frac{\alpha_{AB}Q^n}{Q^n+\tau^n}}$ always holds. Thus, any solution on the line $A = 1$ will either stay on the boundary or point toward the interior of the state space.

Thus having proved the following result

Theorem 2.1. *The state space Ω is invariant with respect to all solutions of the system* (1)-(2) *with initial conditions in Ω.*

2.2.2. *Phase plane analysis of the 2D model.* We use a phase plane model to analyze our two-dimensional system. The phase plane plots a vector field on the A-B plane, where the vector at (a, b) represents the derivatives evaluated at (a, b); that is, $\left(\frac{\mathrm{d}}{\mathrm{d}t}A|_{(a,b)}, \frac{\mathrm{d}}{\mathrm{d}t}B|_{(a,b)}\right)$. We also plot the nullclines, which are the curves for which either $\frac{\mathrm{d}}{\mathrm{d}t}A = 0$ or $\frac{\mathrm{d}}{\mathrm{d}t}B = 0$. The points at which the nullclines intersect are equilibrium points (also called steady states or rest points). By noting the signs of $\frac{\mathrm{d}}{\mathrm{d}t}A$ and $\frac{\mathrm{d}}{\mathrm{d}t}B$ on the nullclines and in the regions between the nullclines, we can determine the "flow" of solutions.

For our phase plane analysis in Figure 2, we used the default parameters given by $r_1 = r_2 = 2$, $s_1 = s_2 = 2$, $Q = 100$, $\tau = 30$, and $\alpha_{AB} = \alpha_{BA} = 0.5$. With these parameters, there is one coexistence equilibrium point that acts as a saddle. We then varied r_2, τ, and α_{BA} on the following domains respectively: $r_2 \in [0.5, 3.5]$, $\tau \in [10, 70]$, and $\alpha_{BA} \in [0.2, 0.8]$. Note that the behavior for r_1 and α_{AB} would mirror the results for r_2 and α_{BA}. These results are presented on Table 1.

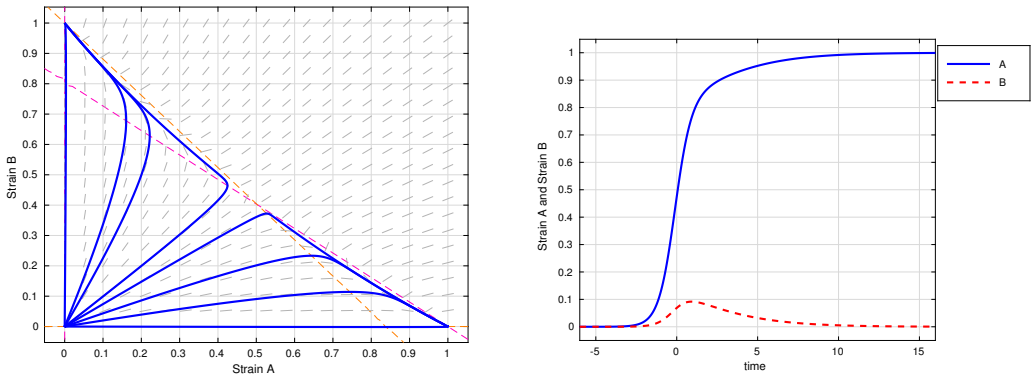

FIGURE 2. Phase plane of Strain A and Strain B (left) and the time plot (right). The time plot shows time in the past, as the solution that goes through the initial conditions has unique values that would lead to those initial conditions if the biofilm was growing in accordance with the model up to that point.

For $r_2 \in (1.5, 2.5)$, the coexistence equilibrium exists, with an advantage for the strain with the higher growth rate. Beyond that range, the strain with the lower growth rate would be eradicated in any mixed environment.

The variation of τ has very little effect on the system. There is always a coexistence equilibrium with equal values for each strain. The only observable change is that the coexistence equilibrium values were slightly higher for each strain as the quorum sensing threshold increased.

Varying α_{BA} always maintains a coexistence equilibrium. The strain with the higher killing rate has an advantage over the other strain, so the coexistence equilibrium is shifted towards the dominant strain.

2.2.3. *Results for Model 1.* The model (1)-(2) can have up to four equilibria, which can be found by setting $\frac{dA}{dt} = 0$, $\frac{dB}{dt} = 0$. Three of these equilibria are located on the boundary of our state space. There is a bacteria-free equilibrium at $(A, B) = (0, 0)$. There is also an equilibrium with only A present at $\left(\frac{r_1}{s_1}, 0\right)$. Similarly, there is an

Changed Parameter Value	Number of Equilibria	Coexistence Equilibrium	Long Term Behavior
$r_2 = 0.5$	3	Does not exist	A dominates
$r_2 = 1$	3	Does not exist	A dominates
$r_2 = 1.5$	3	Does not exist	A dominates
$r_2 = 2$	4	$(0.44678, 0.44678)$	Higher ratio dominates
$r_2 = 2.5$	3	Does not exist	B dominates
$r_2 = 3$	3	Does not exist	B dominates
$r_2 = 3.5$	3	Does not exist	B dominates
$\tau = 10$	4	$(0.44460, 0.44460)$	Higher ratio dominates
$\tau = 20$	4	$(0.44531, 0.44531)$	Higher ratio dominates
$\tau = 30$	4	$(0.44678, 0.44678)$	Higher ratio dominates
$\tau = 40$	4	$(0.44903, 0.44903)$	Higher ratio dominates
$\tau = 50$	4	$(0.45199, 0.45199)$	Higher ratio dominates
$\tau = 60$	4	$(0.45548, 0.45548)$	Higher ratio dominates
$\tau = 70$	4	$(0.45928, 0.45928)$	Higher ratio dominates
$\alpha_{BA} = 0.2$	4	$(0.66876, 0.26750)$	Higher ratio dominates
$\alpha_{BA} = 0.3$	4	$(0.57374, 0.34424)$	Higher ratio dominates
$\alpha_{BA} = 0.4$	4	$(0.50236, 0.40189)$	Higher ratio dominates
$\alpha_{BA} = 0.5$	4	$(0.44678, 0.44678)$	Higher ratio dominates
$\alpha_{BA} = 0.6$	4	$(0.40227, 0.48272)$	Higher ratio dominates
$\alpha_{BA} = 0.7$	4	$(0.36582, 0.51215)$	Higher ratio dominates
$\alpha_{BA} = 0.8$	4	$(0.33543, 0.53670)$	Higher ratio dominates

TABLE 1. One parameter was changed at a time, with the value listed. All changes to growth and killing rate were in (2). To find values if the corresponding parameters in (1) were changed, simply interchange the A and B values of that trial. "Higher ratio dominates" means that the strain of bacteria that has a greater proportion of the biomass than what leads to the coexistence equilibrium dominates.

equilibrium with only B present at $\left(0, \frac{r_2}{s_2}\right)$. Additionally, there is a coexistence equilibrium under certain conditions. The stability of these equilibria are shown below.

Theorem 2.2. *The following statements describe the stability of all equilibria except the coexistence equilibrium:*

(1) The bacteria-free equilibrium at $(0,0)$ *is always unstable.*

(2) The equilibrium with only A present at $\left(\frac{r_1}{s_1}, 0\right)$ *is stable when*

$$r_2 < \left(s_2 - \frac{Q^n}{\tau^n + Q^n}\alpha_{BA}\right)\left(\frac{r_1}{s_1}\right).$$

(3) The equilibrium with only B present at $\left(0, \frac{r_2}{s_2}\right)$ *is stable when*

$$r_1 < \left(s_1 - \frac{Q^n}{\tau^n + Q^n}\alpha_{AB}\right)\left(\frac{r_2}{s_2}\right).$$

Proof. By the Hartman-Grobman Theorem we can show that the stability of the equilibria is similar to the one of its linearization, thus we proceed by linearizing about each equilibrium. Notice that the Jacobian matrix J of the system (1)-(2) is given by

$$J = \begin{pmatrix} r_1 - s_1(2A+B) - \frac{Q^n}{\tau^n+Q^n}\alpha_{AB}B & -s_1A - \frac{Q^n}{\tau^n+Q^n}\alpha_{AB}A \\ -s_2B - \frac{Q^n}{\tau^n+Q^n}\alpha_{BA}B & r_2 - s_2(A+2B) - \frac{Q^n}{\tau^n+Q^n}\alpha_{BA}A \end{pmatrix}.$$

For the bacteria-free equilibrium, we can substitute $A = 0$, $B = 0$ into the matrix, which yields,

$$J|_{(0,0)} = \begin{pmatrix} r_1 & 0 \\ 0 & r_2 \end{pmatrix}.$$

The eigenvalues of this matrix are

$$\lambda_1 = r_1 \quad \lambda_2 = r_2.$$

Because our parameters r_1, r_2 are positive, we know that the equilibrium at $(0,0)$ is an unstable source. Thus proving our first statement.

Next, we substitute the equilibrium $\left(\frac{r_1}{s_1}, 0\right)$ into J. With simplification, this yields

$$J|_{(r_1/s_1,0)} = \begin{pmatrix} -r_1 & -r_1 - \frac{Q^n}{\tau^n+Q^n}\alpha_{AB}\left(\frac{r_1}{s_1}\right) \\ 0 & r_2 - \left(s_2 - \frac{Q^n}{\tau^n+Q^n}\alpha_{BA}\right)\left(\frac{r_1}{s_1}\right) \end{pmatrix}.$$

The eigenvalues for this matrix are

$$\lambda_1 = -r_1 \quad \lambda_2 = r_2 - \left(s_2 - \frac{Q^n}{\tau^n + Q^n}\alpha_{BA}\right)\left(\frac{r_1}{s_1}\right).$$

When λ_2 is negative, both eigenvalues are negative, so there is a stable sink. This occurs when $r_2 < \left(s_2 - \frac{Q^n}{\tau^n + Q^n}\alpha_{BA}\right)\left(\frac{r_1}{s_1}\right)$. Thus proving the second statement. If λ_2 is positive, the eigenvalues have opposite signs so there is an unstable saddle.

Substituting the equilibrium $\left(0, \frac{r_2}{s_2}\right)$ into J gives

$$J|_{(0,r_2/s_2)} = \begin{pmatrix} r_1 - \left(s_1 - \frac{Q^n}{\tau^n+Q^n}\alpha_{AB}\right)\left(\frac{r_2}{s_2}\right) & 0 \\ -r_2 - \frac{Q^n}{\tau^n+Q^n}\alpha_{BA}\left(\frac{r_2}{s_2}\right) & -r_2 \end{pmatrix}.$$

This matrix has the eigenvalues

$$\lambda_1 = r_1 - \left(s_1 - \frac{Q^n}{\tau^n + Q^n}\alpha_{AB}\right)\left(\frac{r_2}{s_2}\right) \quad \lambda_2 = -r_2$$

When λ_1 is positive, there is an unstable saddle. When $r_1 < \left(s_1 - \frac{Q^n}{\tau^n + Q^n}\alpha_{AB}\right)\left(\frac{r_2}{s_2}\right)$, λ_1 is negative, and there is a stable sink. Thus proving the last statement of this theorem. □

Theorem 2.3. *The system* (1)-(6) *has a positive coexistence equilibrium if the following conditions hold:*

(1) $0 \leq r_1 \leq s_1$
(2) $0 \leq r_2 \leq s_2$
(3) Q *is nonzero*
(4) At least one of $s_1\alpha_{BA}$, $s_2\alpha_{AB}$, *and* $\alpha_{AB}\alpha_{BA}$ *is nonzero.*

Proof. Based on the governing equations of the model, a coexistence equilibrium (A*, B*) will satisfy

$$r_1 - s_1(A^* + B^*) - \alpha_{AB}B^*\frac{Q^n}{Q^n + \tau^n} = 0 \quad \text{and} \quad r_2 - s_2(A^* + B^*) - \alpha_{BA}A^*\frac{Q^n}{Q^n + \tau^n} = 0\,,$$

which can be written as the following linear system:

$$M \cdot \begin{bmatrix} A^* \\ B^* \end{bmatrix} = \begin{bmatrix} \frac{r_1}{d_1} \\ \frac{r_2}{s_2} \end{bmatrix} \tag{5}$$

Where

$$M = \begin{bmatrix} \frac{s_1}{d_1} & 1 \\ \frac{d_2}{s_2} & 1 \end{bmatrix},$$

$d_1 = s_1 + \alpha_{AB}\dfrac{Q^n}{Q^n + \tau^n}$, and $d_2 = s_2 + \alpha_{BA}\dfrac{Q^n}{Q^n + \tau^n}$. Recall that our domain is $\Omega = \{(A, B) \in \mathbb{R}^2 : 0 \leq A \leq 1, 0 \leq B \leq 1\}$. We want to formulate restrictions on certain parameters in order to guarantee the existence and uniqueness of a positive equilibrium within our domain. Consider the following two conditions:

(1) The four intercepts of linear system 5 lie on the boundary of our domain
(2) The matrix M is invertible

These two conditions are sufficient (though not necessary) to guarantee a unique solution to the linear system that lies within our domain of interest. The conditions can be expressed symbolically as follows:

(1) $0 \leq \dfrac{r_1}{d_1} \leq 1$, $0 \leq \frac{r_1}{s_1} \leq 1$, $0 \leq \dfrac{r_2}{d_2} \leq 1$, $0 \leq \frac{r_2}{s_2} \leq 1$

It should be clear to see that $s_1 \leq s_1 + \alpha_{AB}\dfrac{Q^n}{Q^n + \tau^n}$ and that $s_2 \leq s_2 + \alpha_{BA}\dfrac{Q^n}{Q^n + \tau^n}$ because all parameters are non-negative. Thus, the condition

that $r_1 \leq s_1$ guarantees that $r_1 \leq d_1$. Similarly, we know that if $r_2 \leq s_2$, then $r_2 \leq d_2$.

(2)

$$
\begin{aligned}
det(M) = \frac{s_1}{d_1} - \frac{d_2}{s_2} &\neq 0 \\
s_1 s_2 &\neq d_1 d_2 \\
s_1 s_2 &\neq \left(s_1 + \alpha_{AB}\frac{Q^n}{Q^n+\tau^n}\right)\left(s_2 + \alpha_{BA}\frac{Q^n}{Q^n+\tau^n}\right) \\
0 &\neq s_1\alpha_{BA}\frac{Q^n}{Q^n+\tau^n} + s_2\alpha_{AB}\frac{Q^n}{Q^n+\tau^n} + \alpha_{AB}\alpha_{BA}\left(\frac{Q^n}{Q^n+\tau^n}\right)^2
\end{aligned}
$$

□

Theorem 2.4. *The positive equilibrium of the system* (1)-(2) *is stable when*

$$\max\{r_1, r_2\} < \min\{Re(\lambda_{V_0}), Re(\lambda_{V_1})\}\,,$$

where λ_{V_0} *and* λ_{V_1} *represent the eigenvalues of the matrix*

$$V = \begin{bmatrix} 2s_1A + d_1B & d_1A \\ d_2B & 2s_2B + d_2A \end{bmatrix}.$$

The positive equilibrium is unstable when

$$\max\{r_1, r_2\} > \min\{Re(\lambda_{V_0}), Re(\lambda_{V_1})\}\,.$$

Proof. We can express the Jacobian of the system (1)-(2) as a difference of a diagonal matrix and a positive real-valued matrix; we have $J = D - V$ where

$$D = \begin{bmatrix} r_1 & 0 \\ 0 & r_2 \end{bmatrix} \quad \text{and} \quad V = \begin{bmatrix} 2s_1A + d_1B & d_1A \\ d_2B & 2s_2B + d_2A \end{bmatrix}.$$

We are interested in a positive equilibrium; in other words, $0 < A \leq 1$ and $0 < B \leq 1$. Let λ_{V_0} and λ_{V_1} represent the eigenvalues of matrix V, and let λ_{J_0} and λ_{J_1} represent the eigenvalues of matrix J. We have that the real part of each of the eigenvalues of J will lie in the following ranges as a result of adding a multiple of the corresponding identity matrix:

$$
\begin{aligned}
\min\{r_1, r_2\} - \mathrm{Re}(\lambda_{V_0}) \leq \mathrm{Re}(\lambda_{J_0}) \leq \max\{r_1, r_2\} - \mathrm{Re}(\lambda_{V_0}) \\
\min\{r_1, r_2\} - \mathrm{Re}(\lambda_{V_1}) \leq \mathrm{Re}(\lambda_{J_1}) \leq \max\{r_1, r_2\} - \mathrm{Re}(\lambda_{V_1}).
\end{aligned}
$$

We wish to formulate a set of conditions on our parameters that will yield a stable or unstable positive equilibrium. A stable positive equilibrium is guaranteed if the real part of the corresponding eigenvalues of the Jacobian matrix are negative, that is, $\mathrm{Re}(\lambda_{J_0}) < 0$ and $\mathrm{Re}(\lambda_{J_1}) < 0$, from the Hartman-Grobman theorem and the linear stability of an autonomous dynamical system we know that the local stability of the equilibria is that of their corresponding linearization. Assuming $\mathrm{Re}(\lambda_{V_0})$ and $\mathrm{Re}(\lambda_{V_1})$ are non-negative, then the necessary set of conditions will be $\max\{r_1, r_2\} - \mathrm{Re}(\lambda_{V_0}) < 0$ and $\max\{r_1, r_2\} - \mathrm{Re}(\lambda_{V_1}) < 0$; more simply, these conditions can be expressed by $\max\{r_1, r_2\} < \min\{\mathrm{Re}(\lambda_{V_0}), \mathrm{Re}(\lambda_{V_1})\}$. So all that remains is to prove that $\mathrm{Re}(\lambda_{V_0})$ and $\mathrm{Re}(\lambda_{V_1})$ are non-negative. The full expressions for λ_{V_0} and λ_{V_1} are as follows:

$$\lambda_{V_0} = \frac{Ad_2 + Bd_1 + 2As_1 + 2Bs_2 + \sqrt{d}}{2}$$
$$\lambda_{V_1} = \frac{Ad_2 + Bd_1 + 2As_1 + 2Bs_2 - \sqrt{d}}{2},$$

where

$$\begin{aligned} d =& A^2{d_2}^2 - 4A^2d_2s_1 + 4A^2{s_1}^2 + 2ABd_1d_2 + 4ABd_1s_1 + 4ABd_2s_2 - 8ABs_1s_2 \\ &+ B^2{d_1}^2 - 4B^2d_1s_2 + 4B^2{s_2}^2 . \end{aligned}$$

If $d < 0$, it is immediate that $\mathrm{Re}(\lambda_{V_0}) = \mathrm{Re}(\lambda_{V_1}) = \dfrac{Ad_2 + Bd_1 + 2As_1 + 2Bs_2}{2} \geq 0$, because all parameters are non-negative and $A, B > 0$. If $d \geq 0$, it is clear that λ_{V_0} will be non-negative. So our final step is to prove that λ_{V_1} is non-negative, given that $\sqrt{d}$ is real. Symbolically, we aim to show that

$$Ad_2 + Bd_1 + 2As_1 + 2Bs_2 - \sqrt{d} \geq 0, \quad \text{or}$$
$$Ad_2 + Bd_1 + 2As_1 + 2Bs_2 \geq \sqrt{d}.$$

Squaring both sides and combining like terms, we arrive at the following:

$$6A^2d_2s_1 + 6B^2d_1s_2 + 2A^2s_1d_2 + 4ABs_1s_2 + 2B^2d_1s_2 + 12ABs_1s_2 \geq 0$$

which must be true because all parameters are non-negative and $A, B > 0$.
Thus, the positive equilibrium of our 2D ODE system will be stable as long as $\max\{r_1, r_2\} < \min\{\mathrm{Re}(\lambda_{V_0}), \mathrm{Re}(\lambda_{V_1})\}$. Moreover, by an analogous argument we have that the positive equilibrium is unstable if $\max\{r_1, r_2\} > \min\{\mathrm{Re}(\lambda_{V_0}), \mathrm{Re}(\lambda_{V_1})\}$. □

τ	(A^*, B^*)	$\min\{\lambda_{V_0}, \lambda_{V_1}\}$
10	(0.4446, 0.4446)	1.7784
20	(0.4453, 0.4453)	1.7812
30	(0.4468, 0.4468)	1.7871
40	(0.4490, 0.4490)	1.7961
50	(0.4520, 0.4520)	1.8079
60	(0.4555, 0.4555)	1.8219
70	(0.4593, 0.4593)	1.8371

TABLE 2. Positive equilibrium values of the 2D system and minimum eigenvalues of V are given for various values of τ. Values have been rounded to four decimal places. The minimum eigenvalues can be used to evaluate the stability of the equilibrium using Theorem 2.4

For base values of our parameters (found in Table 3), we have $\max\{r_1, r_2\} = \max\{2, 2\} = 2$. Table 2 shows the value of $\min\{\lambda_{V_0}, \lambda_{V_1}\}$ for all the values of τ we are considering. Since $\max\{r_1, r_2\} = 2 > \min\{\lambda_{V_0}, \lambda_{V_1}\}$ for all values of τ, Theorem 2.4 tells us that the positive equilibrium of the system (1)-(2) is always unstable. Using the stability of the four equilibria, we are able to describe the end behavior of solutions to the system (1)-(2).

Proposition 2.5. *The system* (1)-(2) *is a competitive system.*

Proof. This proposition follows from Definition 6.2, since the off-diagonal entries of the Jacobian matrix are less than or equal to zero for all points in the state space Ω. □

Theorem 2.6. *The solution of the system* (1)-(2) *for any initial condition in the state space converges to one of the four equilibria.*

Proof. Consider an arbitrary point $P \in \Omega$. If we view P as an initial condition and the orbit of P as the corresponding solution to the 2D system, the Poincare-Bendixson theorem tells us the following about this initial-value problem: either

(1) P is an equilibrium point,
(2) The solution to the initial value problem converges to an equilibrium, or

(3) The solution to the initial value problem leads to a limit cycle.

We focus our attention on the third option; that is, we must show that all bounded solutions of a competitive system converge to an equilibrium. We have that our state space is a compact set; since Ω is in $\mathbb{R}^2$, it is closed and bounded. Thus all solutions to the 2D system must converge to an equilibrium by Theorem 6.6. Using what we have proved about the stability of the four equilibria, we know the following:

(1) Since the origin is an unstable source, only the initial condition (0,0) can converge to the origin.
(2) Since the coexistence equilibrium is an unstable saddle point, there exists a line of points that converge to this equilibrium. This line is the stable manifold of the equilibrium, and splits the state space into two disjoint connected sections.
(3) The single-strain equilibria are both stable, and both correspond to one of the connected sections produced by the stable manifold of the coexistence equilibrium. Loosely speaking, this implies that solutions starting in the upper half of the state space will converge to the equilibrium at $(0, B^*)$, while solutions starting in the lower half of the state space will converge to the equilibrium at $(A^*, 0)$.

This proves that any solution to the 2D system that starts within the state space will converge to one of the four equilibria. □

Symbol	Parameter	Source	Value	Units
r_1	basal growth rate of strain A	[14]	2	d^{-1}
r_2	basal growth rate of strain B	[14]	2	d^{-1}
s_1	mortality rate for strain A	[14]	2	d^{-1}
s_2	mortality rate for strain B	[14]	2	d^{-1}
n	degree of polymerization	[8]	2.5	-
τ	quorum sensing induction threshold	[7]	10-70	nM
α_{AB}	rate at which strain B kills strain A using T6SS	[14]	0.5	d^{-1}
α_{BA}	rate at which strain A kills strain B using T6SS	[14]	0.5	d^{-1}
β_1	constitutive autoinducer production rate	[7]	0.5520	nMd^{-1}
β_2	induced autoinducer production rate	[7]	5.520	nMd^{-1}
δ	biomass motility coefficient	[7]	10^{-12}	m^2d^{-1}
a	biofilm diffusion exponent	[7]	4	-
b	biofilm diffusion exponent	[7]	4	-

TABLE 3. Parameter values are drawn from [7], [8], and [14]. Time is measured in days, concentrations are given in nanomoles, and space is represented in meters.

2.3. **Model 2 - Extended ODE model with production of autoinducer.**

2.3.1. *Standard ODE model without Quorum Sensing degradation.* Model 2 includes a third differential equation for the production rate of the autoinducer. We used ideas from [7] to formulate (8). The autoinducer is produced at a base rate β_1 if the local concentration is small relative to the induction threshold. The production rate increases to $\beta_1 + \beta_2$ once the concentration exceeds the threshold. With Q as a variable rather than a parameter, this model is able to demonstrate the effect of the increasing concentration of the autoinducer. In other words, the regulatory effect of quorum sensing on T6SS mediated killing is captured well in this three-dimensional ODE model.
The model reads as follows:

$$\frac{\mathrm{d}}{\mathrm{d}t}A = r_1 A - s_1 A(A+B) - \frac{Q^n}{\tau^n + Q^n}\alpha_{AB} AB \tag{6}$$

$$\frac{\mathrm{d}}{\mathrm{d}t}B = r_2 B - s_2 B(A+B) - \frac{Q^n}{\tau^n + Q^n}\alpha_{BA} AB \tag{7}$$

$$\frac{\mathrm{d}}{\mathrm{d}t}Q = \left(\beta_1 + \beta_2 \frac{Q^n}{\tau^n + Q^n}\right)(A+B) \tag{8}$$

The schematic diagram in Figure 3 illustrates the interactions among the three dependent variables - A, B, and Q - in Model 2.

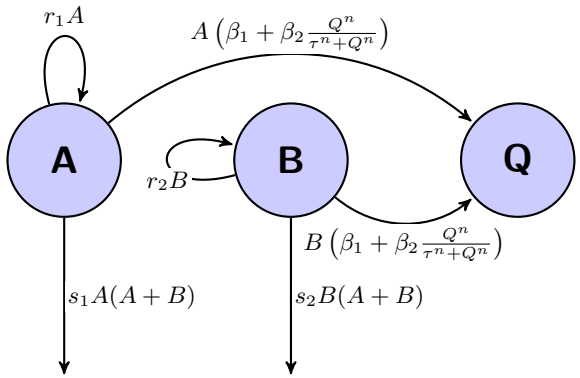

FIGURE 3. Schematic diagram for the 3D ODE model

To non-dimensionalize this model we will rescale t and Q. Let T and q be dimensionless variables such that $T = \frac{t}{\delta}$ and $q = \frac{Q}{\gamma}$, where δ and γ are scaling parameters. By substituting for the respective variables and applying the chain rule as needed, the model now reads

$$\frac{\mathrm{d}}{\mathrm{d}T}A = \delta\left(r_1 A - s_1 A(A+B) - \frac{\gamma^n q^n}{\tau^n + \gamma^n q^n}\alpha_{AB} AB\right) \tag{9}$$

$$\frac{\mathrm{d}}{\mathrm{d}T}B = \delta\left(r_2 B - s_2 B(A+B) - \frac{\gamma^n q^n}{\tau^n + \gamma^n q^n}\alpha_{BA} AB\right) \tag{10}$$

$$\frac{\mathrm{d}}{\mathrm{d}T}q = \frac{\delta}{\gamma}\left(\beta_1 + \beta_2 \frac{\gamma^n q^n}{\tau^n + \gamma^n q^n}\right)(A+B) \tag{11}$$

where $\gamma = \tau$ and $\delta = \dfrac{1}{r_1 + r_2}$

2.3.2. *Local stability of equilibria of the system* (6)-(8).

Theorem 2.7. *The following statements describe the equilibria of Model 2.*

(1) The system (6)-(8) *does not have a coexistence equilibrium.*

(2) The Q-axis represents a collection of infinitely many non-hyperbolic equilibria.

Proof. Observe that when A and B are nonzero, $\frac{\mathrm{d}}{\mathrm{d}t}Q$ is positive and non-decreasing. Thus it is impossible for the concentration of autoinducer molecules to achieve a steady state. We conclude that there does not exist an equilibrium where A, B, and Q are all positive. This proves Statement 1.

The Q-axis can be defined as the set of points $\{(A, B, Q) \in \mathbb{R}^3 : A = 0, B = 0, Q \in \mathbb{R}\}$. Note that any point on the Q-axis results in $\dfrac{\mathrm{d}}{\mathrm{d}t}A = \dfrac{\mathrm{d}}{\mathrm{d}t}B = \dfrac{\mathrm{d}}{\mathrm{d}t}Q = 0$ and thus represents an equilibrium of the system. Recall that a non-hyperbolic equilibrium is characterized by a Jacobian matrix that has at least one eigenvalue with real part equal to zero. On the Q-axis, the Jacobian matrix for the system becomes

$$J = \begin{bmatrix} r_1 & 0 & 0 \\ 0 & r_2 & 0 \\ \beta_1 + \frac{Q^n \beta_2}{Q^n + \tau^n} & \beta_1 + \frac{Q^n \beta_2}{Q^n + \tau^n} & 0 \end{bmatrix}.$$

The spectrum of J is $\{0, r_1, r_2\}$; it follows that any point on the Q-axis represents a non-hyperbolic equilibrium. This proves Statement 2. □

The inquiry for the non-degradation of Quorum Sensing (QS) can incite further studies to its relationship to the extinction of both strain of bacteria through the T6SS killing as the accumulation of QS molecules increases with respect of time. But the possibility of chemical decay of QS through several processes is still an aspect to be studied

2.3.3. *Standard ODE model with Quorum Sensing degradation.* Exact mechanisms for the decay of autoinducer molecules is a current area of study. When a term representing the decay of autoinducer molecules is included on (6)-(8), allows the possibility of a positive equilibrium. The model now reads as follows:

$$\frac{\mathrm{d}}{\mathrm{d}t}A = r_1 A - s_1 A(A+B) - \frac{Q^n}{\tau^n + Q^n}\alpha_{AB} AB \tag{12}$$

$$\frac{\mathrm{d}}{\mathrm{d}t}B = r_2 B - s_2 B(A+B) - \frac{Q^n}{\tau^n + Q^n}\alpha_{BA} AB \tag{13}$$

$$\frac{\mathrm{d}}{\mathrm{d}t}Q = \left(\beta_1 + \beta_2 \frac{Q^n}{\tau^n + Q^n}\right)(A+B) - \lambda Q \tag{14}$$

2.3.4. *Equilibria of the system* (12)-(14). The model (12)-(14) equilibria can be found by finding the solutions to the nonlinear system $\frac{dA}{dt} = 0$, $\frac{dB}{dt} = 0$, $\frac{dQ}{dt} = 0$. Without much effort we can observe that there is a bacteria-free equilibrium at $A = 0$, $B = 0$, $Q = 0$. Nevertheless, a key difference with respect to the model (1)-(2), the single-strain and coexistence equilibria depend on the positive solutions of the following function of Q

$$\left\{\beta_1 + \beta_2 \frac{Q^n}{\tau^n + Q^n}\right\} P - \lambda Q = 0 \tag{15}$$

Where $P \in (0, 1]$ on the single strain equilibria and $P > 0$ for the coexistence equilibrium. First let us remark the following:

Corollary 2.8. *The equation given in* (15) *has at least one positive solution if* $P \in (0, 1]$.

Proof. Let us notice since $\tau > 0$ and $n > 0$ for most biologically relevant cases we have that the solutions of (15) when $P \in (0, 1]$. Notice that the function $f(Q) = \left\{\beta_1 + \beta_2 \frac{Q^n}{\tau^n + Q^n}\right\} P - \lambda Q$ is continuous for any $Q \geq 0$, its such that $f(0) > 0$ and

$f(t) < 0$ for a sufficiently large $t > 0$, therefore by Bolzano's theorem we know that a root for $f(Q)$ exists. □

The previous result allows us to observe that when $A = \frac{r_1}{s_1}$, $B = 0$ there is at least one single-strain equilibrium for some $Q > 0$. A similar argument follows when $A = 0$, $B = \frac{r_2}{s_2}$, and some $Q > 0$ holds a different single-strein equilibrium. Moreover the possibility of a coexistence equilibrium, that is $A, B, Q > 0$, can be guaranteed under the following conditions.

From this result, we can establish the following conjecture with respect to the coexistence equilibrium solution of the system (12)-(14)

Conjecture 2.9. *The existence of the coexistence equilibria depends on the parameters of the system* (12)-(14) *in sense of not only the solution of* $\frac{\mathrm{d}}{\mathrm{d}t}Q = 0$ *but that such solution holds the conditions established in Theorem* 2.3

The base of the previous conjecture relies on repeated numerical experimentation where parameters were variated from the nominal values. The equilibria were obtained on each case and during several occurences no coexistence equilibria were found regardless of solving $\frac{\mathrm{d}}{\mathrm{d}t}Q = 0$ when $A \neq 0$ and $B \neq 0$.

2.3.5. *Stability of the equilibria for the system* (12)-(14). The stability of these equilibria are analyzed below.

Theorem 2.10. *The following statements describe the stability of all boundary equilibria of the system* (12)-(14)*:*

(1) The bacteria-free equilibrium is always unstable.

(2) If $r_2 s_1(Q^n + \tau^n) > Q^n \alpha_{BA} r_1$*, then the single-strain equilibrium where A dominates is stable as long as*

$$\min\left\{r_1, \frac{r_1 s_2}{s_1}, \lambda\right\} > \max\left\{\lambda_{V_0}, \lambda_{V_1}, \lambda_{V_2}\right\} .$$

If $r_2 s_1(Q^n + \tau^n) > Q^n \alpha_{BA} r_1$*, then this equilibrium will be unstable if*

$$\min\left\{r_1, \frac{r_1 s_2}{s_1}, \lambda\right\} < \max\left\{\lambda_{V_0}, \lambda_{V_1}, \lambda_{V_2}\right\} .$$

(3) *If* $r_1 s_2(Q^n+\tau^n) > Q^n \alpha_{AB} r_2$*, then the single-strain equilibrium where* B *dominates is stable as long as*

$$\min\left\{\frac{r_2 s_1}{s_2}, r_2, \lambda\right\} > \max\left\{\lambda_{V_0}, \lambda_{V_1}, \lambda_{V_2}\right\} .$$

If $r_1 s_2(Q^n+\tau^n) > Q^n \alpha_{AB} r_2$*, then this equilibrium will be unstable if*

$$\min\left\{\frac{r_2 s_1}{s_2}, r_2, \lambda\right\} < \max\left\{\lambda_{V_0}, \lambda_{V_1}, \lambda_{V_2}\right\} .$$

Proof. We begin by analyzing the bacteria-free equilibrium. The Jacobian matrix of the system evaluated at $(0,0,0)$ is given by

$$J_0 = \begin{bmatrix} r_1 & 0 & 0 \\ 0 & r_2 & 0 \\ \beta_1 + \frac{Q^n\beta_2}{Q^n+\tau^n} & \beta_1 + \frac{Q^n\beta_2}{Q^n+\tau^n} & -\lambda \end{bmatrix} .$$

The spectrum of J_0 is $\{r_1, r_2, -\lambda\}$. Since r_1 and r_2 are positive, we know that the equilibrium at $(0,0,0)$ is an unstable node. This proves statement 1.

We now consider the single-strain equilibrium where A dominates, which occurs at $\left(\frac{r_1}{s_1}, 0, Q\right)$, where $Q > 0$. The Jacobian matrix of the system evaluated at such equilibrium is given by

$$J = \begin{bmatrix} -r_1 & -r_1 - \frac{Q^n\alpha_{AB}r_1}{s_1(Q^n+\tau^n)} & 0 \\ 0 & r_2 - \frac{r_1 s_2}{s_1} - \frac{Q^n\alpha_{BA}r_1}{s_1(Q^n+\tau^n)} & 0 \\ \beta_1 + \frac{Q^n\beta_2}{Q^n+\tau^n} & \beta_1 + \frac{Q^n\beta_2}{Q^n+\tau^n} & \frac{r_1}{s_1}\left(\frac{Q^{n-1}\beta_2 n}{Q^n+\tau^n} - \frac{Q^{2n-1}\beta_2 n}{(Q^n+\tau^n)^2}\right) - \lambda \end{bmatrix} .$$

We can rewrite J as a difference between a real-valued matrix V and a diagonal matrix D so that $J = V - D$, where

$$V = \begin{bmatrix} -r_1 & -\frac{Q^n\alpha_{AB}r_1}{s_1(Q^n+\tau^n)} & 0 \\ 0 & r_2 - \frac{Q^n\alpha_{BA}r_1}{s_1(Q^n+\tau^n)} & 0 \\ \beta_1 + \frac{Q^n\beta_2}{Q^n+\tau^n} & \beta_1 + \frac{Q^n\beta_2}{Q^n+\tau^n} & \frac{r_1}{s_1}\left(\frac{Q^{n-1}\beta_2 n}{Q^n+\tau^n} - \frac{Q^{2n-1}\beta_2 n}{(Q^n+\tau^n)^2}\right) \end{bmatrix} ,$$

and

$$D = \begin{bmatrix} r_1 & 0 & 0 \\ 0 & \frac{r_1 s_2}{s_1} & 0 \\ 0 & 0 & \lambda \end{bmatrix} .$$

Let λ_{V_0}, λ_{V_1}, and λ_{V_2} represent the eigenvalues of matrix V, and let λ_{J_0}, λ_{J_1}, and λ_{J_2} represent the eigenvalues of matrix J. We have that the real part of each of the eigenvalues of J will lie in the following ranges as a result of adding a multiple of the corresponding identity matrix:

$$\begin{aligned}
&\mathrm{Re}(\lambda_{V_0}) - \max\left\{r_1, \frac{r_1 s_2}{s_1}, \lambda\right\} \leq \mathrm{Re}(\lambda_{J_0}) \leq \mathrm{Re}(\lambda_{V_0}) - \max\left\{r_1, \frac{r_1 s_2}{s_1}, \lambda\right\} \\
&\mathrm{Re}(\lambda_{V_1}) - \max\left\{r_1, \frac{r_1 s_2}{s_1}, \lambda\right\} \leq \mathrm{Re}(\lambda_{J_1}) \leq \mathrm{Re}(\lambda_{V_1}) - \max\left\{r_1, \frac{r_1 s_2}{s_1}, \lambda\right\} \\
&\mathrm{Re}(\lambda_{V_1}) - \max\left\{r_1, \frac{r_1 s_2}{s_1}, \lambda\right\} \leq \mathrm{Re}(\lambda_{J_1}) \leq \mathrm{Re}(\lambda_{V_1}) - \max\left\{r_1, \frac{r_1 s_2}{s_1}, \lambda\right\}.
\end{aligned}$$

We wish to formulate a set of conditions on our parameters that will yield a stable or unstable positive equilibrium. A stable positive equilibrium is guaranteed if $\mathrm{Re}(\lambda_{J_0}) < 0$, $\mathrm{Re}(\lambda_{J_1}) < 0$, and $\mathrm{Re}(\lambda_{J_2}) < 0$, from the Hartman-Grobman theorem and the linear stability of an autonomous dynamical system. Assuming $\mathrm{Re}(\lambda_{V_0})$, $\mathrm{Re}(\lambda_{V_1})$, $\mathrm{Re}(\lambda_{V_2})$ are non-negative, then the necessary set of conditions will be

$$\mathrm{Re}(\lambda_{V_0}) - \min\left\{r_1, \frac{r_1 s_2}{s_1}, \lambda\right\} < 0\,,$$

$$\mathrm{Re}(\lambda_{V_1}) - \min\left\{r_1, \frac{r_1 s_2}{s_1}, \lambda\right\} < 0\,,$$

and

$$\mathrm{Re}(\lambda_{V_2}) - \min\left\{r_1, \frac{r_1 s_2}{s_1}, \lambda\right\} < 0\,;$$

more simply, these conditions can be expressed as

$$\min\left\{r_1, \frac{r_1 s_2}{s_1}, \lambda\right\} > \max\{\mathrm{Re}(\lambda_{V_0}), \mathrm{Re}(\lambda_{V_1}), \mathrm{Re}(\lambda_{V_2})\}\,.$$

This condition rests upon the assumption that all eigenvalues of V are nonnegative. The spectrum of V is given by

$$\left\{0, \frac{Q^n \beta_2 n r_1 \tau^n}{Q^{2n+1} s_1 + Q s_1 \tau^{2n} + 2Q^{n+1} s_1 \tau^n}, \frac{Q^n r_2 s_1 - Q^n \alpha_{BA} r_1 + r_2 s_1 \tau^n}{s_1 (Q^n + \tau^n)}\right\}.$$

Obviously 0 is nonnegative, and $\dfrac{Q^n \beta_2 n r_1 \tau^n}{Q^{2n+1} s_1 + Q s_1 \tau^{2n} + 2Q^{n+1} s_1 \tau^n}$ must also be nonnegative since all parameter values are nonnegative. To ensure the third eigenvalue is nonnegative, we need to have $r_2 s_1 (Q^n + \tau^n) \geq Q^n \alpha_{BA} r_1$. If we consider biologically

relevant values for these parameters (i.e. $1 \leq r_1, r_2, s_1, s_2 \leq 3$, $0 \leq \alpha_{BA} \leq 1$, $n = 2.5$, $10 \leq \tau \leq 70$), as well as a range for Q that is consistent with MATLAB equilibrium simulations ($0 < Q \leq 2$), then this condition on the third eigenvalue always holds. We have shown that if $r_2 s_1 (Q^n + \tau^n) > Q^n \alpha_{BA} r_1$, then this single-strain equilibrium is stable as long as

$$\min\left\{r_1, \frac{r_1 s_2}{s_1}, \lambda\right\} > \max\{\lambda_{V_0}, \lambda_{V_1}, \lambda_{V_2}\}.$$

By an analogous argument, the equilibrium will be unstable if

$$\min\left\{r_1, \frac{r_1 s_2}{s_1}, \lambda\right\} < \max\{\lambda_{V_0}, \lambda_{V_1}, \lambda_{V_2}\}.$$

This proves Statement 2.

Lastly we consider the single-strain equilibrium where B dominates, which occurs at $\left(0, \frac{r_2}{s_2}, Q\right)$, where $Q > 0$. The Jacobian matrix of the system evaluated at $\left(0, \frac{r_1}{s_1}, Q\right)$ is

$$J = \begin{bmatrix} r_1 - \frac{r_2 s_1}{s_2} - \frac{Q^n \alpha_{AB} r_2}{s_2(Q^n+\tau^n)} & 0 & 0 \\ -r_2 - \frac{Q^n \alpha_{BA} r_2}{s_2(Q^n+\tau^n)} & -r_2 & 0 \\ \beta_1 + \frac{Q^n \beta_2}{Q^n+\tau^n} & \beta_1 + \frac{Q^n \beta_2}{Q^n+\tau^n} & \frac{r_2}{s_2}\left(\frac{Q^{n-1}\beta_2 n}{Q^n+\tau^n} - \frac{Q^{2n-1}\beta_2 n}{(Q^n+\tau^n)^2}\right) - \lambda \end{bmatrix}.$$

We can rewrite J as a difference between a real-valued matrix V and a diagonal matrix D so that $J = V - D$, where

$$V = \begin{bmatrix} r_1 - \frac{Q^n \alpha_{AB} r_2}{s_2(Q^n+\tau^n)} & 0 & 0 \\ -\frac{Q^n \alpha_{BA} r_2}{s_2(Q^n+\tau^n)} & -r_2 & 0 \\ \beta_1 + \frac{Q^n \beta_2}{Q^n+\tau^n} & \beta_1 + \frac{Q^n \beta_2}{Q^n+\tau^n} & \frac{r_2}{s_2}\left(\frac{Q^{n-1}\beta_2 n}{Q^n+\tau^n} - \frac{Q^{2n-1}\beta_2 n}{(Q^n+\tau^n)^2}\right) \end{bmatrix}$$

and

$$D = \begin{bmatrix} \frac{r_2 s_1}{s_2} & 0 & 0 \\ 0 & r_2 & 0 \\ 0 & 0 & \lambda \end{bmatrix}.$$

Let λ_{V_0}, λ_{V_1}, and λ_{V_2} represent the eigenvalues of matrix V, and let λ_{J_0}, λ_{J_1}, and λ_{J_2} represent the eigenvalues of matrix J. We have that the real part of each of the

eigenvalues of J will lie in the following ranges as a result of adding a multiple of the corresponding identity matrix:

$$\mathrm{Re}(\lambda_{V_0}) - \max\left\{\frac{r_2 s_1}{s_2}, r_2, \lambda\right\} \leq \mathrm{Re}(\lambda_{J_0}) \leq \mathrm{Re}(\lambda_{V_0}) - \max\left\{\frac{r_2 s_1}{s_2}, r_2, \lambda\right\}$$
$$\mathrm{Re}(\lambda_{V_1}) - \max\left\{\frac{r_2 s_1}{s_2}, r_2, \lambda\right\} \leq \mathrm{Re}(\lambda_{J_1}) \leq \mathrm{Re}(\lambda_{V_1}) - \max\left\{\frac{r_2 s_1}{s_2}, r_2, \lambda\right\}$$
$$\mathrm{Re}(\lambda_{V_1}) - \max\left\{\frac{r_2 s_1}{s_2}, r_2, \lambda\right\} \leq \mathrm{Re}(\lambda_{J_1}) \leq \mathrm{Re}(\lambda_{V_1}) - \max\left\{\frac{r_2 s_1}{s_2}, r_2, \lambda\right\}.$$

We wish to formulate a set of conditions on our parameters that will yield a stable or unstable positive equilibrium. A stable positive equilibrium is guaranteed if $\mathrm{Re}(\lambda_{J_0}) < 0$, $\mathrm{Re}(\lambda_{J_1}) < 0$, and $\mathrm{Re}(\lambda_{J_2}) < 0$, from the Hartman-Grobman theorem and the linear stability of an autonomous dynamical system. Assuming $\mathrm{Re}(\lambda_{V_0})$, $\mathrm{Re}(\lambda_{V_1})$, and $\mathrm{Re}(\lambda_{V_2})$ are non-negative, then the necessary set of conditions will be $\mathrm{Re}(\lambda_{V_0}) - \min\left\{\frac{r_2 s_1}{s_2}, r_2, \lambda\right\} < 0$, $\mathrm{Re}(\lambda_{V_1}) - \min\left\{\frac{r_2 s_1}{s_2}, r_2, \lambda\right\} < 0$, and $\mathrm{Re}(\lambda_{V_2}) - \min\left\{\frac{r_2 s_1}{s_2}, r_2, \lambda\right\} < 0$; more simply, these conditions can be expressed as

$$\min\left\{\frac{r_2 s_1}{s_2}, r_2, \lambda\right\} > \max\left\{\mathrm{Re}(\lambda_{V_0}), \mathrm{Re}(\lambda_{V_1}), \mathrm{Re}(\lambda_{V_2})\right\}.$$

This condition rests upon the assumption that all eigenvalues of V are nonnegative. The spectrum of V is given by

$$\left\{0, \frac{Q^n \beta_2 n r_2 \tau^n}{Q^{2n+1} s_2 + Q s_2 \tau^{2n} + 2Q^{n+1} s_2 \tau^n}, \frac{Q^n r_1 s_2 - Q^n \alpha_{AB} r_2 + r_1 s_2 \tau^n}{s_2(Q^n + \tau^n)}\right\}.$$

Obviously 0 is nonnegative, and $\frac{Q^n \beta_2 n r_2 \tau^n}{Q^{2n+1} s_2 + Q s_2 \tau^{2n} + 2Q^{n+1} s_2 \tau^n}$ must also be nonnegative since all parameter values are nonnegative. To ensure the third eigenvalue is nonnegative, we need to have $r_1 s_2(Q^n + \tau^n) \geq Q^n \alpha_{AB} r_2$. Note that if we consider biologically relevant values for these parameters (i.e. $1 \leq r_1, r_2, s_1, s_2 \leq 3$, $0 \leq \alpha_{AB} \leq 1$, $n = 2.5$, $10 \leq \tau \leq 70$), as well as a range for Q that is consistent with MATLAB equilibrium simulations ($0 < Q \leq 2$), then this condition on the third eigenvalue always holds. We have shown that if $r_1 s_2(Q^n + \tau^n) \geq Q^n \alpha_{AB} r_2$ holds, then this single-strain equilibrium is stable as long as $\min\left\{\frac{r_2 s_1}{s_2}, r_2, \lambda\right\} > \max\{\mathrm{Re}(\lambda_{V_0}), \mathrm{Re}(\lambda_{V_1}), \mathrm{Re}(\lambda_{V_2})\}$. By an analogous argument, if $r_1 s_2(Q^n + \tau^n) \geq Q^n \alpha_{AB} r_2$ holds, then this equilibrium

will be unstable if $\min\left\{\frac{r_2 s_1}{s_2}, r_2, \lambda\right\} < \max\{\mathrm{Re}(\lambda_{V_0}), \mathrm{Re}(\lambda_{V_1}), \mathrm{Re}(\lambda_{V_2})\}$. This proves Statement 3. □

Conjecture 2.11. *The coexistence equilibrium for the system* (12)-(14)*, when exists, is unstable.*

As previously mentioned, repeated numerical experimentation were effectuated and when the existence of a positive equilibrium was established the corresponding eigenvalues of the Jacobian matrix were obtained. On each case, the existence of a positive eigenvalue was encountered, thus aiming for the conjecture above.

2.4. **Computational Realizations for model 2.** We solve Model 2 using ODE-solving software in MATLAB. MATLAB contains a number of different ODE solvers which are designed to accommodate different types of systems. The ode45 solver has medium accuracy and is generally a good first choice. However, using ode45 produced oscillations in the solution curve for strain B which were not consistent with the biology underlying our model. This suggests that we might have a stiff model, where "stiff" is used to describe an ODE problem that is difficult to evaluate for some reason. An example of a stiff problem is one in which the equations in the system vary on drastically different time scales. Based on our issues with ode45, we decided to use ode23s, which is better suited to stiff problems.

2.4.1. *Effect of quorum sensing regulated T6SS killing.* Figure 4 shows the relationship between different values of τ and various other aspects of Model 2. In figures 4a and 4b the fractional volume of the biofilm for each bacterial strain is shown with respect to time and different values for τ. When τ is larger the time it takes for the two strains to reach equilibrium is longer. In figure 4c the effects of varying τ on various measures of T6SS related killing can be seen, where the larger the value of τ is the longer it takes for T6SS killing to reach its full expression. Lastly 4d shows that as the value of τ increases, the concentration of the autoinducer is slower to increase.

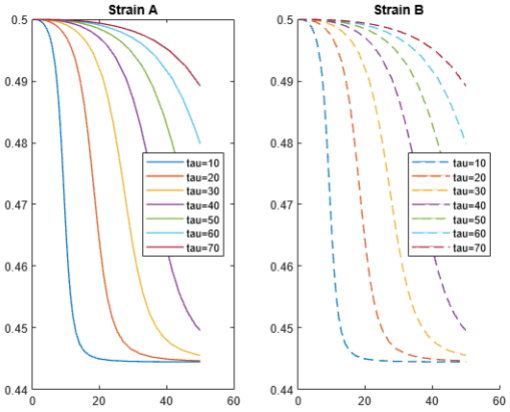

(A)

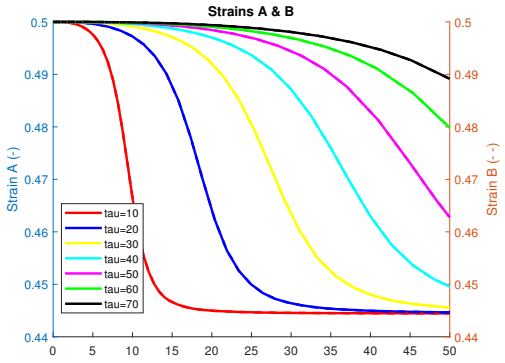

(B)

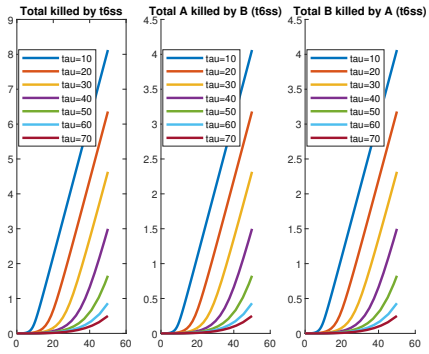

(C)

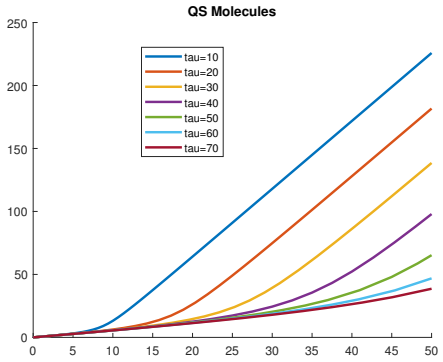

(D)

FIGURE 4. Solutions of Model 2 using McNally's parameters with varying τ

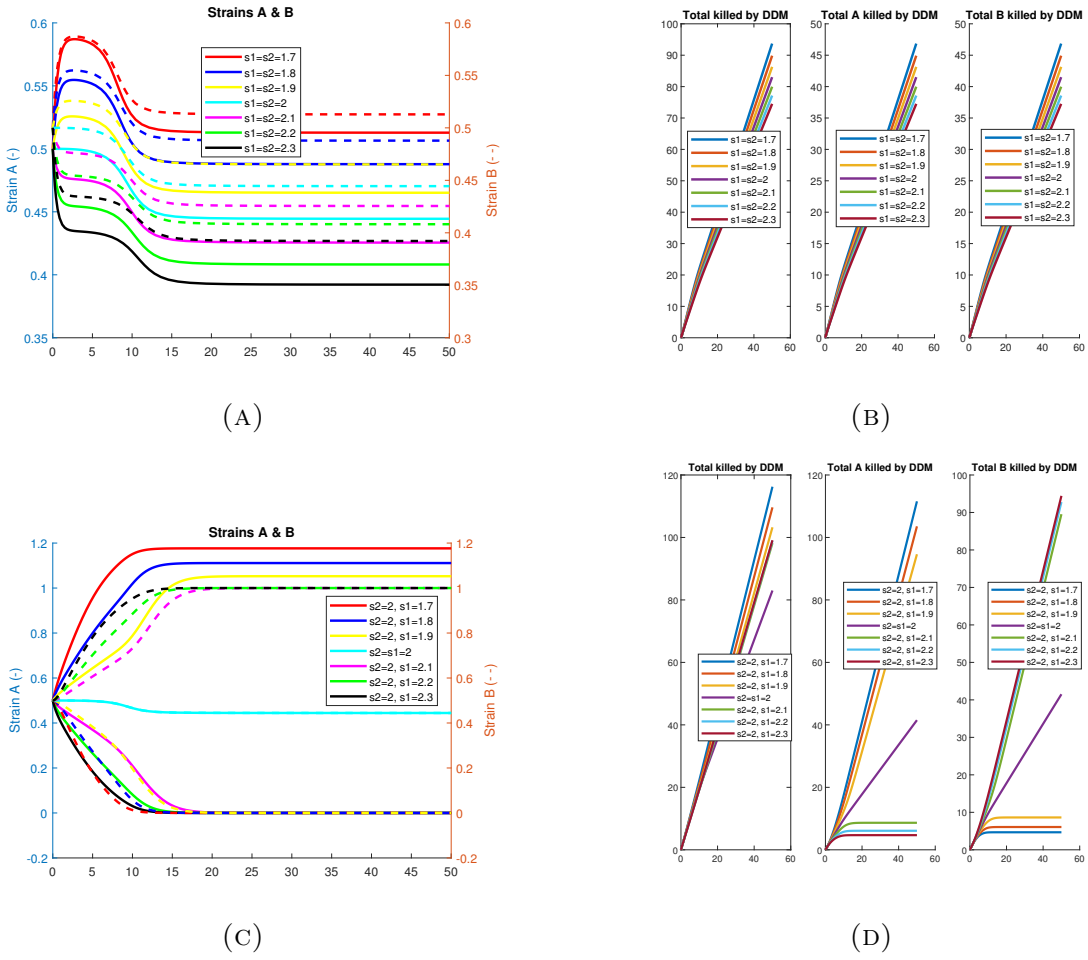

FIGURE 5. Solutions of Model 2 using McNally's parameters with varying density dependant mortality values

2.4.2. *Effect of density dependent T6SS killing.* Figure 5 shows the effects of density dependant mortality (DDM) on the biofilm. DDM is the death rate of the two bacterial strains caused by factors that relate to the current volume of the biofilm that is occupied which is expressed by the s_1 and s_2 terms in Model 2. Some forms of death in DDM are expressed T6SS killing and natural death rates. Figure 5a shows the effects on bacterial strains A and B when $s_1 = s_2$ and the value of the rates range from 1.7 to 2.3. Figure 5b deals with the same s_1 and s_2 as in 5a and tracks the different amount of killing done by DDM in the biofilm. In Figure 5c and 5d we

hold s_2 constant at 2 and vary s_1 between 1.7 and 2.3 to see the effects that this has on the strains A and B and the amount of DDM related killing respectively.

3. Discussion

The novelty of this project lies in its ability to capture the effect of quorum sensing on T6SS-mediated killing in the bacterial species *Agrobacterium tumefaciens*. To this end, we have constructed two ODE models that reflect the interplay of these biological processes in order to discern possible benefits to the biofilm and effects on the biofilm structure.

The 2D Model

The two-dimensional ODE system models the volume fractions of strains A and B over time, with Q included as a constant. In this sense, the 2D model can be viewed as a snapshot of a specific point in the quorum sensing process.

The value of the quorum sensing threshold τ had negligible effect on the behavior of the system. This makes sense because the quorum sensing term $\dfrac{Q^n}{Q^n + \tau^n}$ is composed of constants, so it does not change with time. Thus the quorum sensing term is effectively absorbed into the killing rate, increasing the amount of T6SS-mediated killing. If we had defined the quorum sensing term differently, or chosen a different value for Q, perhaps we would have observed different behavior.

Conversely, the growth and density-dependent mortality rates of the strains had very large impacts on the system. As Table 1 shows, growth rates that differ by more than 0.5 result in a guaranteed single-strain equilibrium. Plot (d) in Figure 5 illustrates that density-dependent mortality rates that differ by as little as 0.1 can result in significantly greater biomass loss for the strain with higher mortality. Since two strains of the same bacterial species are more likely to have similar growth and mortality rates than two completely different species, this suggests that a biofilm composed of multiple strains of the same bacterial species may be more likely to achieve a state of coexistence than a biofilm that consists of completely different bacterial species.

To reiterate, the 2D model provides a snapshot in time, so it cannot help us answer questions about the development of the biofilm over time, or about the effects of quorum sensing on the structure and life cycle of the biofilm. However, the simplicity of the model allows us to observe the effects of individual parameters. We can use

this knowledge as we construct our 3D ODE model, which is more complex but more biologically relevant than the 2D model.

The 3D Model

In our 3D model, quorum sensing was treated as a dependent variable rather than an independent variable, increasing the complexity of the system. All other factors were unchanged from the 2D model.

Similar to the 2D model, the coexistence equilibrium of the system is unstable. It is important to clarify what an unstable equilibrium means for a biological system. An unstable equilibrium does not imply that all solutions will move away from the equilibrium; there exists a section of the domain such that solutions in this section will converge to the equilibrium. However, to ensure the existence and stability of the positive equilibrium, we found that the model parameters must have very specific relationships. This suggests that in reality, the coexistence equilibrium will rarely be achieved. The instability of the positive equilibrium, combined with the complicated parameter conditions, indicates that we are unlikely to have a single positive coordinate of volume fractions (A^*, B^*) that endures over time.

With the addition of a separate differential equation modeling quorum sensing, the quorum sensing threshold began to have a much more noticeable effect on the behavior of the system. When we varied τ in the 2D system, it had a negligible effect on the system; however, varying τ in the 3D system markedly changed the trajectories of the solution curves. Increasing the quorum sensing threshold decreased the amount of T6SS-mediated killing and increased the time for solutions to reach equilibrium. By controlling the time it takes the biofilm to experience the full effects of T6SS killing, quorum sensing plays a significant regulatory role in the development of the biofilm. The quorum sensing threshold works as a control on the system; increasing τ means there is more time for the strains to grow without the full influence of the T6SS killing, while decreasing τ means that killing will reach its full expression early in the growth phase, and so the complete eradication of one strain is more likely. It seems that manipulating the quorum sensing process (by either decreasing the quorum sensing threshold or increasing the production rate of the autoinducer) is an effective way to reduce a multi-strain/multi-species biofilm to a mono-strain/mono-species biofilm. Once the biofilm has been reduced to a single strain or species, it is easier to eradicate the whole biofilm. Different bacterial strains or species may have

different tolerances to an antibiotic treatment, so a multi-strain/multi-species biofilm could require multiple different treatments. On the other hand, a mono-strain/mono-species biofilm could be wiped out with just one antibiotic treatment. Our research findings suggest that exploiting quorum sensing regulation of T6SS-mediated killing is a natural, low-cost way to remove harmful biofilms from plant hosts.

While changing τ affects the time it takes the system to reach its full expression of T6SS killing, we did not find any evidence that τ is a bifurcation parameter; that is, varying τ within a biologically relevant range (provided by [7]) did not affect the existence or stability of any of our equilibria. This indicates that quorum sensing regulation of T6SS killing is a robust mechanism that transcends specific details of the quorum sensing process.

The biggest drawback of our models is the lack of experimental data with which to compare our findings. However, we can consult existing published results to corroborate the accuracy of our results. One relevant result comes from Gallique, et. al. ([9]). The researchers concluded that T6SS-mediated killing can serve as an indirect form of communication and social interaction, in the sense that the amount of T6SS killing can provide an overall view of bacterial density. Our results support and clarify Gallique's conclusion; indeed, T6SS can be viewed as an indirect form of cell-to-cell communication, and it is made possible by the direct response of the bacterial cells to increasing concentrations of the autoinducer.

4. Future Directions

The most natural extension of this research project would be an analysis of our PDE model. We initially developed a system of partial differential equations by adding a diffusion term to each equation in our 3D ODE model. However, computational difficulties prohibited us from doing a full mathematical analysis of this model. Since the PDE model is able to capture the spatial distribution of A, B, and Q within the biofilm, it can provide insight that our ODE models cannot. One of our motivating research questions was related to the physical structure and development of the biofilm; in this sense, analysis of a PDE model would be a very valuable addition to this research project. Perhaps simulations of the PDE model could reveal spatial patterns or trends over time that help explain or clarify the results that we derived from our two ODE models.

Another immediate concern that has arisen upon completion of this project is related to experimental data. The base parameter values presented in Table 3 are all supported by existing literature; however, we varied these values when we conducted a sensitivity analysis on Model 1 and when we performed simulations of Model 2. We defined the domains on which we varied the base parameter values, so supporting evidence is needed to prove that these domains are biologically reasonable. In a broader sense, we could not find any published experimental results that were directly relevant to our project. Although much research has been done on biofilms, the relationship between quorum sensing and T6SS-mediated killing has not been extensively studied. In addition, because we restricted our focus to *Agrobacterium tumefaciens*, there are no experimental papers that we know of that speak to our specific research question. Although the absence of relevant experimental data means that our conclusions must be mostly speculative, this does not imply that our results are not valuable. Experimental studies related to quorum sensing in bacteria are notoriously time-consuming and expensive, so experimenters could benefit from looking to mathematical modeling results like ours in order to pose more well-informed research questions.

5. Conclusion

By constructing mathematical models that capture the effect of quorum sensing on T6SS-mediated killing in the bacterial species *Agrobacterium tumefaciens*, we were able to show that when using biologically relevant parameter values an unstable coexistence equilibrium will occur. The instability of this equilibrium suggests that T6SS-mediated killing controlled by quorum sensing drives competition in multi strain or multi specie biofilms. Even though T6SS-mediated killing seems to drive competition it is still possible that during the growth stage of the biofilm both strains could amass at similar rates and together reach an unstable coexistence. Because of the type of equilibrium that our models show, in a real world setting it may be expected that a single strain will out compete the other and drive it to extinction within the biofilm rather than ever reaching any type of cooperation.

6. Appendix

6.1. Relevant Theorems.

Theorem 6.1 (**Hartman-Grobman Theorem**). *Consider the autonomous system of ordinary differential equations*

$$x' = f(x) \tag{16}$$

where f is continuously differentiable in an open subset $D \subset \mathbb{R}^n$. If x_0 is a hyperbolic rest point for the autonomous differential equation (16) then there is an open set U containing x_0 and a homeomorphism H with domain U such that the orbits of the differential equation 16 are mapped by H to orbits of the linearized system $x' = Df(x_0)(x - x_0)$ in the set U.

Definition 6.2. Cooperative and Competitive Systems A dynamical system is cooperative if $\frac{\partial f_i}{\partial x_j}(x) \geq 0, i \neq j,\ x \in D$. We say the system is competitive if $\frac{\partial f_i}{\partial x_j}(x) \leq 0, i \neq j,\ x \in D$.

Definition 6.3 (**Kamke condition** cf. [17] p. 32)**.** Given the system (16) we say that f is of type K in D if for each i, $f_i(a) \leq f_i(b)$ for any two points a and b in D satisfying $a \leq b$ and $a_i = b_i$.

Theorem 6.4 (**Kamke's Theorem** cf. [17], p. 32)**.** *Let f be type K on D and $x_0, y_0 \in D$. Let $<_r$ denote one any of the relations $\leq$, $<$ or $<<$. If $x_0 <_r y_0$, $t > 0$ and $\phi_t(x_0)$ and $\phi_t(y_0)$ are defined, then $\phi_t(x_0) <_r \phi_t(y_0)$.*

Theorem 6.5 (cf. [18], p.268)**.** *Let $\pi(x, t)$ denote the dynamical system generated by the autonomous system of differential equations (16). If (16) is cooperative in D, then π is a monotone dynamical system with respect to $\leq$ in D. If (16) is cooperative and irreducible in D, then π is a strongly monotone system with respect to $\leq$ in D.*

Theorem 6.6 (cf. [17], p. 35)**.** *All bounded solutions of a cooperative system in $\mathbb{R}^2$ converge to an equilibrium point.*

Theorem 6.7. Generalized Poincaré-Bendixson Theorem *Let M be a positively invariant region for the vector field generated by (16) in $\mathbb{R}^2$ and where the*

vector field has a finite number of fixed points. Let $p \in M$, and consider $\omega(p)$. Then one of the following possibilities holds.

- *$\omega(p)$ is a fixed point;*
- *$\omega(p)$ is a closed orbit;*
- *$\omega(p)$ consists of a finite number of fixed points $p_1, \ldots, p_n$ and orbits γ with $\alpha(\omega) = p_i$ and $\omega(\gamma) = p_j$.*

References

[1] Rhea G Abisado, Saida Benomar, Jennifer R Klaus, Ajai A Dandekar, and Josephine R Chandler. Bacterial quorum sensing and microbial community interactions. *MBio*, 9(3), 2018.

[2] Luke P Allsopp, Patricia Bernal, Laura M Nolan, and Alain Filloux. Causalities of war: The connection between type vi secretion system and microbiota. *Cellular microbiology*, 22(3):e13153, 2020.

[3] Christophe S Bernard, Yannick R Brunet, Erwan Gueguen, and Eric Cascales. Nooks and crannies in type vi secretion regulation. *Journal of bacteriology*, 192(15):3850–3860, 2010.

[4] Graciela Brelles-Marino and Eulogio J Bedmar. Detection, purification and characterisation of quorum-sensing signal molecules in plant-associated bacteria. *Journal of Biotechnology*, 91(2-3):197–209, 2001.

[5] Yassin Cherrak, Nicolas Flaugnatti, Eric Durand, Laure Journet, and Eric Cascales. Structure and activity of the type vi secretion system. *Protein Secretion in Bacteria*, pages 329–342, 2019.

[6] Chandrani Das, Anirban Dutta, Hannah Rajasingh, and Sharmila S Mande. Understanding the sequential activation of type iii and type vi secretion systems in salmonella typhimurium using boolean modeling. *Gut pathogens*, 5(1):28, 2013.

[7] Blessing O Emerenini, Burkhard A Hense, Christina Kuttler, and Hermann J Eberl. A mathematical model of quorum sensing induced biofilm detachment. *PloS one*, 10(7):e0132385, 2015.

[8] Mallory R Frederick, Christina Kuttler, Burkhard A Hense, and Hermann J Eberl. A mathematical model of quorum sensing regulated eps production in biofilm communities. *Theoretical Biology and Medical Modelling*, 8(1):8, 2011.

[9] Mathias Gallique, Mathilde Bouteiller, and Annabelle Merieau. The type vi secretion system: a dynamic system for bacterial communication? *Frontiers in microbiology*, 8:1454, 2017.

[10] Mathias Gallique, Victorien Decoin, Corinne Barbey, Thibaut Rosay, Marc GJ Feuilloley, Nicole Orange, and Annabelle Merieau. Contribution of the pseudomonas fluorescens mfe01 type vi secretion system to biofilm formation. *PLoS One*, 12(1):e0170770, 2017.

[11] Bijay K Khajanchi, Jian Sha, Elena V Kozlova, Tatiana E Erova, Giovanni Suarez, Johanna C Sierra, Vsevolod L Popov, Amy J Horneman, and Ashok K Chopra. N-acylhomoserine lactones involved in quorum sensing control the type vi secretion system, biofilm formation, protease production, and in vivo virulence in a clinical isolate of aeromonas hydrophila. *Microbiology*, 155(Pt 11):3518, 2009.

[12] áB Lesic, áM Starkey, J He, R Hazan, and LG Rahme. Quorum sensing differentially regulates pseudomonas aeruginosa type vi secretion locus i and homologous loci ii and iii, which are required for pathogenesis. *Microbiology*, 155(Pt 9):2845, 2009.

[13] Charlotte Majerczyk, Emily Schneider, and E Peter Greenberg. Quorum sensing control of type vi secretion factors restricts the proliferation of quorum-sensing mutants. *Elife*, 5:e14712, 2016.

[14] Luke McNally, Eryn Bernardy, Jacob Thomas, Arben Kalziqi, Jennifer Pentz, Sam P Brown, Brian K Hammer, Peter J Yunker, and William C Ratcliff. Killing by type vi secretion drives genetic phase separation and correlates with increased cooperation. *Nature communications*, 8(1):1–11, 2017.

[15] Peter M Merritt, Thomas Danhorn, and Clay Fuqua. Motility and chemotaxis in agrobacterium tumefaciens surface attachment and biofilm formation. *Journal of bacteriology*, 189(22):8005–8014, 2007.

[16] Kai Papenfort and Bonnie L Bassler. Quorum sensing signal–response systems in gram-negative bacteria. *Nature Reviews Microbiology*, 14(9):576, 2016.

[17] Hal L. Smith. *Monotone Dynamical Systems. An Introduction to the Theory of Competitive and Cooperative Systems*. Mathematical Surveys and Monographs. American Mathematical Society, 1995.

[18] Paul Waltman and Hal L. Smith. *The Theory of the Chemostat: Dynamics of Microbial Competition*. Number 13 in Cambridge Studies in Mathematical Biology. Cambridge University Press, 1995.

[19] Barbara Weber, Medisa Hasic, Chang Chen, Sun Nyunt Wai, and Debra L Milton. Type vi secretion modulates quorum sensing and stress response in vibrio anguillarum. *Environmental microbiology*, 11(12):3018–3028, 2009.

[20] Chih-Feng Wu, Jer-Sheng Lin, Gwo-Chyuan Shaw, and Erh-Min Lai. Acid-induced type vi secretion system is regulated by exor-chvg/chvi signaling cascade in agrobacterium tumefaciens. *PLoS Pathog*, 8(9):e1002938, 2012.

[21] Liyang Xiong, Robert Cooper, and Lev S Tsimring. Coexistence and pattern formation in bacterial mixtures with contact-dependent killing. *Biophysical journal*, 114(7):1741–1750, 2018.

[22] Weipeng Zhang, Shengjuan Xu, Jing Li, Xihui Shen, Yao Wang, and Zhiming Yuan. Modulation of a thermoregulated type vi secretion system by ahl-dependent quorum sensing in yersinia pseudotuberculosis. *Archives of Microbiology*, 193(5):351–363, 2011.

[23] Jun Zheng, Ok S Shin, D Ewen Cameron, and John J Mekalanos. Quorum sensing and a global regulator tsra control expression of type vi secretion and virulence in vibrio cholerae. *Proceedings of the National Academy of Sciences*, 107(49):21128–21133, 2010.

Colorado College
E-mail address: a_ezell@coloradocollege.edu

Oregon State University
E-mail address: nesheimd@oregonstate.edu

Lewis and Clark College
E-mail address: ksweet@lclark.edu